Molecular Biology of the Cell
Vol. 16, 1258–1267, March 2005

Carbohydrate- and Conformation-dependent Cargo Capture for ER-Exit[D]

Christian Appenzeller-Herzog,*† Beat Nyfeler,* Peter Burkhard,‡ Inigo Santamaria,§‖ Carlos Lopez-Otin,§ and Hans-Peter Hauri*

*Department of Pharmacology and Neurobiology and ‡M. E. Müller Institute for Structural Biology, Biozentrum, University of Basel, CH-4056 Basel, Switzerland; and §Departamento de Bioquimica y Biologia Molecular, Instituto Universitario de Oncologia, Universidad de Oviedo, 33006-Oviedo, Spain

Submitted August 17, 2004; Revised November 22, 2004; Accepted December 16, 2004
Monitoring Editor: Reid Gilmore

Some secretory proteins leave the endoplasmic reticulum (ER) by a receptor-mediated cargo capture mechanism, but the signals required for the cargo-receptor interaction are largely unknown. Here, we describe a novel targeting motif that is composed of a high-mannose type oligosaccharide intimately associated with a surface-exposed peptide β-hairpin loop. The motif accounts for lectin ERGIC-53–assisted ER-export of the lyososomal enzyme procathepsin Z. The second oligosaccharide chain of procathepsin Z exhibits no binding activity for ERGIC-53, illustrating the selective lectin properties of ERGIC-53. Our data suggest that the conformation-based motif is only present in fully folded procathepsin Z and that its recognition by ERGIC-53 reflects a quality control mechanism that acts complementary to the primary folding machinery in the ER. A similar oligosaccharide/β-hairpin loop structure is present in cathepsin C, another cargo of ERGIC-53, suggesting the general nature of this ER-exit signal. To our knowledge this is the first documentation of an ER-exit signal in soluble cargo in conjunction with its decoding by a transport receptor.

INTRODUCTION

A complex interplay between the glycosylation machinery and the deciphering of carbohydrate signals by lectins ensures proper synthesis and targeting of nascent glycoproteins in the secretory pathway of eukaryotic cells. N-linked oligosaccharides are cotranslationally attached to a consensus-site asparagine side chain during translocation of the polypeptide into the ER and may subsequently be processed by numerous glycosidases and glycosyltransferases in ER and Golgi (Kornfeld and Kornfeld, 1985). N-glycans are initially trimmed in the ER from $Glc_3Man_9GlcNAc_2$ to the high-mannose configuration $Man_{7-9}GlcNAc_2$. Later conversion to hybrid- or complex-type oligosaccharides, initiated by the action of Golgi α1,2-mannosidase I, can occur during passage through the Golgi.

Many N-glycan structural intermediates generated during oligosaccharide maturation are thought to serve as signaling tags for quality control, degradation, ER-export, Golgi-to-plasma membrane transport, or lysosomal delivery. The tags are decoded by specific intracellular lectins such as calnexin/calreticulin, EDEM, ERGIC-53, Vip36, or the mannose 6-phospate receptors (Hauri *et al.*, 2000a; Dahms and Hancock, 2002; Ellgaard and Helenius, 2003). Most of these lectins direct their binding solely against a defined carbohydrate motif on the surface of the glycoprotein. In contrast, the fact that transport of only a subset of glycoproteins depends on the mannose-specific lectin ERGIC-53 suggests the presence of a pivotal proteinaceous determinant in these glycoproteins for selective recognition (Hauri *et al.*, 2000b). So far, the search for such additional motifs has remained without success.

One of the functions of ERGIC-53 is to capture transport-competent secretory glycoproteins in the ER and guide them through the COPII pathway to the ERGIC where dissociation occurs triggered by a pH-switch (Appenzeller *et al.*, 1999; Appenzeller-Herzog *et al.*, 2004). Although the glycoproteins proceed through the secretory pathway, ERGIC-53 is recycled back to the ER. This capture mechanism is thought to accelerate the delivery of a number of glycoproteins to post-ER compartments, although its physiological relevance has been demonstrated only for the secretion of blood coagulation factors V and VIII (Nichols *et al.*, 1998).

The lysosomal glycoprotein cathepsin Z (catZ; also named cathepsin X, P, or Y) is ubiquitously expressed and belongs to the papain family of cysteine proteases. It is synthesized in the ER as a preproprotein before the hydrophobic signal peptide is cleaved to release procathepsin Z (procatZ). ProcatZ is a monomer featuring an unusually short propeptide (Santamaria *et al.*, 1998) that is linked into the active site of the enzyme by a disulfide bond (Sivaraman *et al.*, 2000) and cleaved upon lysosomal maturation to produce the active enzyme that remains monomeric. Activated catZ has been purified from human liver (Klemencic *et al.*, 2000). It func-

This article was published online ahead of print in *MBC in Press* (http://www.molbiolcell.org/cgi/doi/10.1091/mbc.E04–08–0708) on January 5, 2005.

[D] The online version of this article contains supplemental material at *MBC Online* (http://www.molbiolcell.org).

Present addresses: †Institute of Biochemistry, ETH Zurich, CH-8093 Zurich, Switzerland; ‖Bone and Mineral Research Unit, Hospital Universitario Central de Asturias, 33006 Oviedo, Spain.

Address correspondence to: Hans-Peter Hauri (Hans-Peter.Hauri@unibas.ch).

Abbreviations used: catZ, cathepsin Z; catZr, cathepsin Z–related protein; DSP, dithiobis(succinimidylpropionate); endoH, endoglycosidase H; ER, endoplasmic reticulum; procatZ, procathepsin Z; wt, wild-type.

© 2005 by The American Society for Cell Biology

tions as a carboxymonopeptidase, although in some cases it also exhibits dipeptidase and endopeptidase activity (Sakamoto *et al.*, 1999; Therrien *et al.*, 2001).

In a previous study, by using the cleavable cross-linker dithiobis (succinimidylpropionate [DSP]), we have identified a specific cargo protein for ERGIC-53 that was dubbed cathepsin Z–related protein (catZr) based on short peptide sequences matching the protein sequence of human procatZ (Appenzeller *et al.*, 1999). In the current study we show that catZr is the Chinese hamster ortholog of human catZ and describe a novel targeting motif in catZ. Teaming up with a specific oligosaccharide, this peptide motif is essential for efficient ERGIC-53–mediated ER export.

MATERIALS AND METHODS

Antibodies

The following antibodies were used: monoclonal antibody (mAb) 9E10.2 against a c-myc epitope (ATCC CRL 1729), mAb G1/93 against human ERGIC-53 (Schweizer *et al.*, 1988), mAb 16B12 against the HA.11-epitope (Covance Research Products, Berkeley, CA), and pAb against Chinese hamster procatZ (anti-catZ; Appenzeller-Herzog *et al.*, 2004). For affinity purification of anti-catZ serum, a 1:1 mixture of the two immunogenic peptides (Figure 1A) including a N-terminal cysteine were coupled to thiol activated Sepharose 4B (Amersham, Piscataway, NJ) as described (Kappeler *et al.*, 1997). The serum was subjected to ammonium sulfate precipitation, dialyzed against phosphate-buffered saline (PBS), and bound to the peptide column overnight. After washing with 20 volumes of PBS and 10 volumes of 10 mM Tris/HCl, pH 7.4, 500 mM NaCl, bound antibodies were eluted sequentially with 10 volumes each of 100 mM glycine/HCl, pH 2.8 and 100 mM triethylamine, pH 11.5. OD_{280} peak-fractions were neutralized with Tris, dialyzed against PBS, and concentrated in a Centriplus YM-30 filter device (Millipore, Bedford, MA).

Screening of a Chinese Hamster Ovary cDNA Library

Based on the sequences of human-, mouse- and rat-preprocathepsin Z cDNAs, we designed degenerate primers corresponding to the catZr peptide sequences (Figure 1B): Coding strand primers 5′-TATCCTCGGCCGCAR-GAGTACC-3′ and 5′-CAGCAYATCCCACAGTAC-3′ and the template strand primer 5′-CCCCAGGGYTCGCCCCATG-3′. Total RNA of GMAA cells was extracted with TRIzol (Invitrogen, Carlsbad, CA), reverse transcribed with MMLV-reverse transcriptase and oligo-dT (Roche, Indianapolis, IN) and used as a template for two PCR reactions with the above primer pairs. The resulting products were [^{32}P]ATP-labeled using a Random Primed DNA labeling kit (Roche) and used to screen a Chinese hamster ovary (CHO) Uni-ZAP XR Lambda cDNA library (Stratagene, La Jolla, CA) according to the manufacturer's instructions and to isolate a cDNA encoding hamster prepro-catZ.

Recombinant DNAs

Insertions or deletions in human prepro-catZ were generated using PCR-based splicing by overlap extension. The 5′-end primer contained a *Bam*HI site before the start ATG, the 3′-end primer a *Xho*I site after the stop codon. The HA-epitope (YPYDVPDYA) was either introduced downstream of the signal peptide cleavage site flanked by two glycins (corresponding to G30) or into the propeptide region by replacing amino acids 50–58. Δloop and Δloop* were produced as depicted in Figure 3A using the HA-tagged cDNAs as template. The resulting cDNAs were cloned into pcDNA 3.1 vector (Invitrogen) via *Bam*HI and *Xho*I sites. Glycosylation-site mutations (changing the codons 184 and/or 224 from AAC to CAG) were introduced by PCR. N184Q+Δloop was generated by the QuikChange method (Stratagene) using the Δloop-cDNA as template.

Cell Culture, Transfection, Drug Treatment, and In Situ Cross-linking

CHO-KI, Lec1, GM, and GMAA cells were cultured as described (Appenzeller-Herzog *et al.*, 2004) and transfected with FuGENE 6 (Roche). Kifunensin (100 μM/Toronto Research Chemicals, North York, Canada) and brefeldin A (10 μg/ml/Epicenter Technologies, Madison WI) were added 60 or 30 min, respectively, before and during the entire pulse-chase period. In situ cross-linking with DSP (Pierce, Rockford, IL) has been described (Appenzeller *et al.*, 1999).

Metabolic Labeling, Immunoprecipitation, and Endoglycosidase Digest

Pulse-chase experiments with [^{35}S]methionine (PerkinElmer, Norwalk, CT) or ^{32}P-orthophosphate (Amersham) and native immunoprecpitations from cell lysates were performed as described (Appenzeller *et al.*, 1999; Nufer *et al.*, 2003). Secreted HA-procatZ was recovered by immunoprecipitation from cell media which, after clearance by a 10-min centrifugation step (20,000 × *g*), had been supplemented with 1% TX-100. Immunoprecipitations using anti-catZ were done after antigen denaturation (Appenzeller-Herzog *et al.*, 2004), and prior treatment of the cells with DSP was required to remove an unspecific 40-kDa band already present in preimmunoprecipitates (Supplementary Figure S1B). For the experiments presented in Figures 1B, 1D, 2C, and 3D, and Supplementary Figures S2 and S3 we used anti-ERGIC-53 immunobeads that had been chemically coupled with dimethyl pimelimidate (Sigma, St. Louis, MO). For ERGIC-53/HA sequential immunoprecipitations, cross-linked anti-ERGIC-53 immunocomplexes were released from the beads and denatured by boiling them for 10 min in 30 mM triethanoamine/HCl, pH 8.1, 100 mM NaCl, 5 mM EDTA, and 1.6% SDS. The resulting supernatant was split for direct analysis (10%) or for subsequent anti-HA immunoprecipitation (90%) after diluting and adjusting the buffer to 2% TX-100. EndoH (Roche) digestion of immunoprecipitates has been described (Kappeler *et al.*, 1997). For PNGase F digestion, the immunobeads were boiled for 3 min in 100 mM $NaPO_4$, pH 7.2, 1% β-mercaptoethanol, 10 mM EDTA, and 0.1% SDS. An equal volume of the same buffer containing 1% TX-100 instead of SDS and protease inhibitors was added, and the sample was digested with 1 U of PNGase F (Roche) at 37°C overnight. Unless stated otherwise, proteins were separated by 10% reducing SDS-PAGE and visualized by Western blotting, phosphorimaging, or fluorography.

RESULTS

ProcatZ Is a Cargo for ERGIC-53

A previous effort to isolate cargo proteins of the ER-export receptor ERGIC-53 from CHO cells resulted in the identification of catZr (Appenzeller *et al.*, 1999). To characterize this protein in more detail, we screened a CHO-cDNA library as illustrated in Supplementary Figure S1A. A partial cDNA of 1334 base pairs length was obtained that includes the start methionine and a poly-A tail and encodes a protein of 306 amino acids with a predicted MW of ~34 kDa and 82% identity to human preprocathepsin Z (Figure 1A). We call this protein Chinese hamster ortholog of procatZ. An anti-peptide rabbit antiserum (Appenzeller-Herzog *et al.*, 2004) readily immunoprecipitated exogenous as well as endogenous catZ (Figure S1B).

Is the hamster procatZ indeed identical to catZr? To test this, we performed DSP-cross-linking and anti-ERGIC-53 immunoprecipitation experiments and probed for the presence of procatZ by immunoblotting using affinity-purified anti-catZ. The experiments were performed in GMAA cells, which derive from Lec1 cells (Stanley *et al.*, 1975) and stably express a myc-tagged, ER-locked, dominant negative GMAA-mutant of ERGIC-53 (Kappeler *et al.*, 1997). GMAA cells are routinely used for cross-linking experiments in the present study, because the overexpression and ER-retention of the mutant ERGIC-53 leads to enhanced cross-linking of cargo proteins to ERGIC-53 (Appenzeller *et al.*, 1999). Figure 1B shows that procatZ as well as mature catZ (after the proteolytic removal of its propeptide; Figure 1A and Supplementary Figure S1B) was detected in cell homogenates, but primarily procatZ was coisolated with GMAA-ERGIC-53 after cross-linking with DSP (the minor fraction of cleaved procatZ is most likely due to a proteolytic event occurring after cell lysis, because cross-linking is performed in situ). The result suggests a specific interaction between procatZ and ERGIC-53. Previously, we have shown that ER-exit of catZr is delayed in GMAA cells compared with cells expressing GM-ERGIC-53, a tagged wild-type (wt) protein (Appenzeller *et al.*, 1999). With this in mind, we studied procatZ maturation in GMAA and GM cells in pulse-chase experiments followed by immunoprecipitation with anti-catZ. Figure 1C shows that procatZ transport is indeed inefficient in GMAA cells. Collectively, these results demonstrate that catZr is identical to the Chinese hamster ortholog of procatZ.

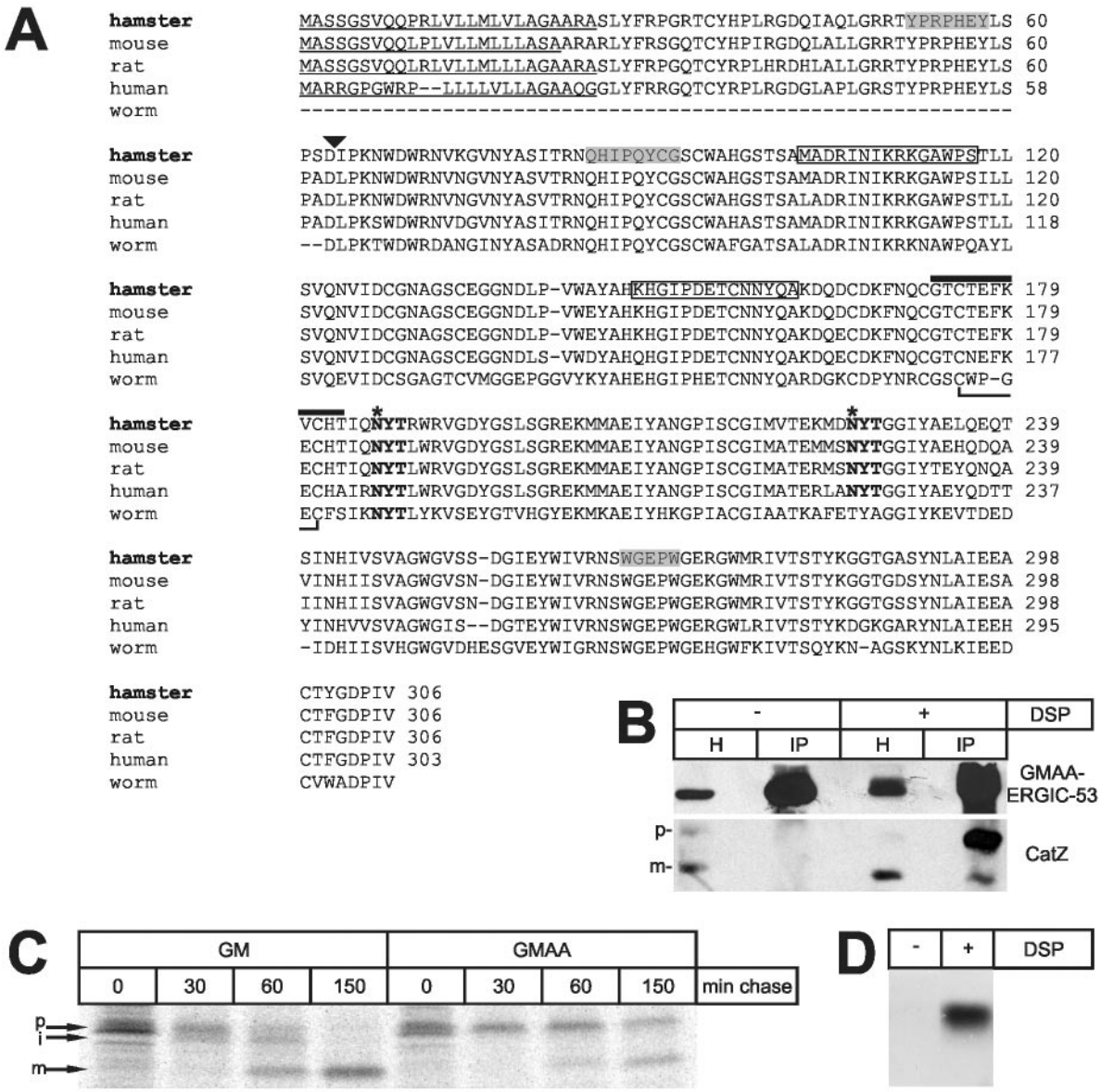

Figure 1. CatZr is the Chinese hamster ortholog of procatZ. (A) Sequence alignment of prepro-catZ from different species. Sequences are available from GenBank/EMBL/DDBJ under accession numbers Q9EPP7 (hamster), Q9WUU7 (mouse), Q9R1T3 (rat), Q9UBR2 (human), NP_491023 (worm). Signal peptides are underlined; the propeptide cleavage site is marked with a triangle; peptides used for immunizing rabbits are boxed; identified catZr-peptides are shaded; glycosylation sites are bold and marked with an asterisk; the two strands of the β-hairpin loop (G_{171}TCNEFKECHA$_{181}$) and the S-S linkage within the loop are indicated by a black bar. (B) Cross-linking and coimmunoprecipitation of GMAA-ERGIC-53 and hamster procatZ. GMAA cells were treated with or without DSP and subjected to anti-ERGIC-53 immunoprecipitation (IP). For comparison, 1% of the total homogenate (H) is shown. GMAA-ERGIC-53 and catZ were visualized by Western blotting (WB) using anti-myc or affinity-purified anti-catZ. Note that procatZ can be cross-linked to ERGIC-53. p, procatZ; m, mature catZ. (C) Maturation of endogenous procatZ in GM and GMAA cells (fluorogram). The cells were pulsed for 15 min with [^{35}S]methionine, chased as indicated, and subjected to anti-catZ immunoprecipitation. p, procatZ; i, intermediate catZ; m, mature catZ. Note that in GMAA cells the transport of catZ is slowed. (D) Coimmunoprecipitation of human procatZ with GMAA-ERGIC-53. GMAA cells were transfected with HA-tagged wt-procatZ cDNA, cross-linked with DSP, and subjected to immunoprecipitation using anti-ERGIC-53 (IP). procatZ was visualized by anti-HA immunoblotting. Note that human procatZ can be coprecipitated with ERGIC-53 in a DSP-dependent way.

To confirm the interaction between procatZ and ERGIC-53, we switched to the human enzyme (Santamaria *et al.*, 1998) that was tagged with a HA-epitope at its N-terminus. GMAA cells were transfected with this construct, cross-linked with DSP, and anti-ERGIC-53 immunoprecipitates were probed by Western blotting for the presence of procatZ using anti-HA. As shown in Figure 1D, human procatZ was coisolated with ERGIC-53 in a DSP-dependent way. Similarly, we were able to cross-link procatZ to endogenous ERGIC-53 in HeLa cells (Supplementary Figure S2). In conjunction with previous control experiments showing the specificity of this cross-linking approach (Appenzeller *et al.*, 1999), these results establish procatZ as a physiological ligand for ERGIC-53.

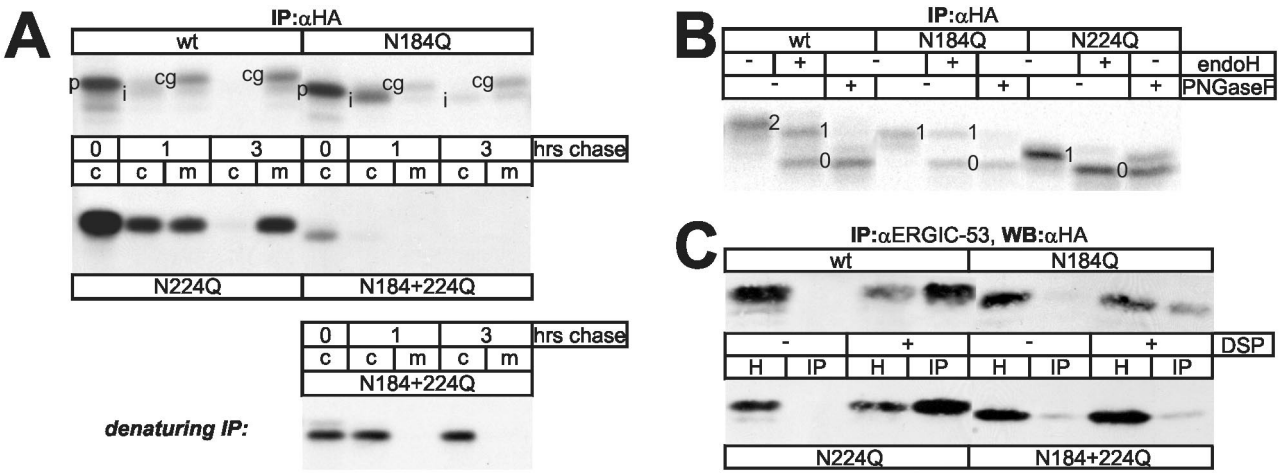

Figure 2. Characterization of procatZ N-glycosylation-site mutants. (A) Top: CHO cells were transfected with wt or glycosylation-site mutant procatZ cDNAs, pulsed for 5 min with [^{35}S]methionine, and chased for the indicated times. Intracellular and secreted procatZ was recovered by anti-HA immunoprecipitation (fluorogram). c, cells; m, medium; p, procatZ; i, intermediate catZ; cg; complex glycosylated catZ. Bottom: pulse-chase analysis as in top panel but using denaturing immunoprecipitation. Note that under these experimental conditions N184 + 224Q is readily detectable. (B) ProcatZ protein secreted from transfected CHO cells after a 5-min pulse and a 3-h chase was isolated by anti-HA immunoprecipitation and subjected to endoH or PNGase F digestion (fluorogram). Numbers indicate doubly-, singly-, and nonglycosylated procatZ. Wt-procatZ and N184Q are partially resistant to endoH, whereas N224Q is almost completely endoH-sensitive. (C) Cross-linking and coimmunoprecipitation of GMAA-ERGIC-53 and procatZ mutants. Anti-ERGIC-53 immunoprecipitates from GMAA-cells expressing the indicated procatZ mutants and treated with or without DSP were analyzed for the presence of procatZ by anti-HA immunoblotting. One percent of the total homogenate (H) was loaded as an expression control. Note that DSP-dependent coisolation is decreased by N184Q, but unaffected by N224Q. IP, immunoprecipitation; WB, Western blotting.

Efficient Transport of procatZ Depends on an ERGIC-53-binding Motif That Is Composed of a High-mannose glycan and a β-hairpin Loop

Binding of procatZ to ERGIC-53 requires N-glycosylation and an active lectin domain in ERGIC-53 (Appenzeller *et al.*, 1999). The sequence of procatZ contains two consensus sites for N-glycosylation at positions 184 and 224 (Figure 1A). To explore the interaction between procatZ and ERGIC-53 in more detail, we generated glycosylation-site mutations N184Q, N224Q, and N184 + 224Q in HA-tagged human procatZ. We first studied their secretion in transiently transfected CHO cells. The cells were pulsed with [^{35}S]methionine, chased for different times and recombinant procatZ was immunoprecipitated from cell lysate or culture medium using anti-HA. The different mutants displayed markedly distinct transport characteristics (Figure 2A). wt- and N224Q-catZ were efficiently secreted, whereas N184Q-catZ was delayed in its secretion (also see Figure 3C). N184 + 224Q could only be recovered efficiently with denaturing immunoprecipitation and was fully retained in the cellular fraction without being degraded. We conclude that the N-linked oligosaccharides of procatZ are specifically required for efficient secretion, but not for intracellular stability of the glycoprotein. It is important to note that in these experiments the mature lysosomal form of catZ is not visible, because the HA-epitope is lost by the proteolytic cleavage of the propeptide (Figure 1A). Furthermore, it must be emphasized that the capacity of intracellular retention and lysosomal targeting of procatZ in CHO cells is already exceeded with endogenous protein levels (Appenzeller-Herzog *et al.*, 2004) and can be virtually neglected, if procatZ is overexpressed (unpublished data).

Next, we examined the carbohydrate processing of the procatZ mutants. In the pulse-chase experiment documented in Figure 2A, a processing intermediate appeared after 1 h of chase with wt- and N184Q-procatZ, but not with N224Q and N184Q + 224Q. This intermediate reflects oligosaccharide trimming by an α1,2-mannosidase (Herscovics, 2001), because it did not appear after treating the cells with kifunensin (unpublished data). Brefeldin A, which leads to relocalization of Golgi enzymes to the ER, induced premature appearance of the trimming intermediate (unpublished data), indicating that this intermediate is generated by the action of Golgi mannosidase I, the only kifunensin-sensitive enzyme in the Golgi. The secreted forms of wt- and N184Q-procatZ exhibited a slower electrophoretic mobility than the intermediate form (Figure 2A) due to complex glycosylation as probed by endoglycosidase H (endoH). They were partially resistant to endoH, but sensitive to PNGase F, which cleaves all forms of N-glycans. Conversely, secreted N224Q remained largely endoH-sensitive (Figure 2B). Thus, complex glycosylation, initiated by Golgi mannosidase I, occurs on a subpopulation of N224-glycans, whereas the major fraction of N184-glycans remains in the high-mannose form.

Because export from the ER is the rate-limiting step for most secretory glycoproteins during exocytosis (Lodish, 1988), the secretion rate of recombinant procatZ constructs is an accurate measure of their efficiency to leave the ER. To test whether the ER-export rate of the three glycosylation mutants of procatZ correlated with their ability to bind ERGIC-53, we transfected GMAA cells with the procatZ mutants, treated them with DSP, immunoprecipitated ERGIC-53, and visualized the mutant proteins by Western blotting using anti-HA. Figure 2C shows that the binding of N184Q and N184 + 224Q to ERGIC-53 was decreased when compared with wt-procatZ, whereas that of N224Q was unaffected. To exclude the trivial possibility that the difference between N184Q and N224Q was due to a steric effect of the N-terminal HA-tag we repeated the cross-linking experiments using a procatZ construct, in which the HA-tag was inserted distal to the N-terminus by replacing a stretch of

flexible amino acids in the propeptide. Coimmunoprecipiations with these alternative mutants gave identical results (Supplementary Figure S3). These data suggest that ERGIC-53 recognizes the N184-glycan of procatZ and that this interaction is largely unchanged in the absence of the N224-glycan.

The surprising selectivity of the N184-glycan for mediating the binding to ERGIC-53 suggested that a carbohydrate-independent determinant may contribute to the recognition of procatZ. This prompted us to look more closely into the structural features of procatZ. We were intrigued by a peptide β-hairpin loop in close proximity of N184 (Sivaraman *et al.*, 2000; Figure 1A), the function of which is unknown. Figure 3A depicts this exposed peptide motif, which comprises a disulfide bond and the high-mannose ($Man_9GlcNAc_2$) N184-glycan that is likely to contact the polar amino acid side chains of the hairpin loop. To study the function of this loop it was shortened (Δloop*) or deleted (Δloop) by mutagenesis (Figure 3A). Cross-linking experiments showed a reduction in the binding of Δloop to ERGIC-53, whereas binding of Δloop* was unaffected (unpublished data). We therefore directed our further efforts to Δloop and, in addition, constructed the combined mutant N184Q+Δloop. Removal of the β-hairpin loop neither affected the intracellular stability (Figure 3B) nor the double glycosylation of procatZ, but slowed its secretion (Figure 3C).

We next examined the role of the hairpin loop in ERGIC-53 binding. The immunoblotting approach in Figure 2C yielded a nonquantitative steady state read-out of the ERGIC-53/procatZ interaction that was critically influenced by mutant-specific transport kinetics. To circumvent this limitation, we studied the interaction of newly synthesized wt and mutant procatZ with ERGIC-53 in GMAA cells by pulse-chase. Because maximal binding of endogenous procatZ to ERGIC-53 occurs after a lag-period of 15 min (Appenzeller *et al.*, 1999), the analysis was performed either immediately after the pulse or after a 15-min chase. The cells were subjected to cross-linking followed by immunoprecipitation using covalently coupled anti-ERGIC-53 (Figure 3D, top panel). Immunocomplexes (comprising both the endogenous hamster and the exogenous human procatZ cross-linked to ERGIC-53) were released form the beads under denaturing conditions and reprecipitated by anti-HA to recover exogenous procatZ only (Figure 3D, bottom panel). Control anti-HA immunoprecipitations from the initial cell lysate showed equal expression levels for all procatZ variants (unpublished data). Quantification of coimmunoprecipitated glycoproteins (Figure 3E) revealed 80% reduction in ERGIC-53 binding of Δloop relative to wt-procatZ. Equal results were obtained for N184Q, and there was no further reduction when both mutations were combined. Unlike with wt and N224Q, we did not observe a lag period for full binding with N184Q, Δloop, and N184Q+Δloop.

With none of the three mutants we observed the lag period for full association described for wt and N224Q.

To corroborate these findings by a different, cross-linking–independent approach, we studied the influence of dominant negative GMAA-ERGIC-53 on the secretion of procatZ mutants. GMAA and Lec1 cells (Lec1 is the parental line of GMAA; Kappeler *et al.*, 1997) were transfected with wt-, N184Q-, N224Q-, and Δloop-procatZ cDNAs, pulse-labeled with [^{35}S]methionine, and chased for 1 h followed by immunoprecipitation of intracellular or secreted procatZ using anti-HA. Figure 4 shows that only the transport of procatZ variants capable of efficiently binding to ERGIC-53 (wt and N224Q) is impaired by ER-localized GMAA-ERGIC-53 in a way similar to endogenous procatZ (Figure 1C).

Although it was likely that the reduced transport rate of N184Q and Δloop arose from their inability to bind to their ER-export receptor ERGIC-53, we also considered the alternative possibility that both the maturation and the ERGIC-53-association of these mutants are impaired because of inefficient folding. Therefore, we assessed intramolecular disulfide formation in procatZ by nonreducing SDS-PAGE. As expected, after a 15-min chase [^{35}S]methionine-labeled, nonreduced wt-procatZ exhibited increased electrophoretic mobility (comparing to its reduced form; Figure 5A), indicating the acquisition of a native conformation. In the pulse-chase experiment in Figure 5B, the process of folding of wt-, Δloop-, and N184Q-procatZ is illustrated by the conversion of a smear (mixed, nonnative disulfides) to a defined band. Although the acquisition of correct intramolecular disulfide bonds in Δloop is at least as efficient as in wt, N184Q exhibits slower folding. We conclude that in the case of Δloop, intracellular transport is impeded because of the absence of an ER-exit signal rather than inefficient protein folding.

The β-hairpin Loop and the N184-glycan Are Intimately Associated

Our finding that the closely apposed N184-glycan and β-hairpin loop equally affected the binding of procatZ to ERGIC-53 (Figure 3E) when deleted separately ("N184Q" and "Δloop") or together ("N184Q+Δloop") suggested that these two elements form a single binding motif composed of carbohydrate and peptide. Alternatively, the two elements may represent two separate low-affinity binding sites and occupation of both binding sites would produce an interaction of higher avidity.

To gain more insight into the interaction between the peptide motif and the N184-glycan, we next focused on the carbohydrate processing in the loop deletion mutants. If the β-hairpin loop, as proposed in Figure 3A, was indeed used like a crook to anchor the highly flexible high-mannose N184-glycan, one would expect that its deletion exposes the N184-glycan to abnormal processing. To test this prediction, we analyzed the sensitivity of secreted Δloop* and Δloop to endoH in CHO cells. As illustrated in Figure 6, Δloop* and, even more drastically, Δloop were far better substrates for the complex glycosylation machinery than the wt enzyme. Obviously, the shortening or absence of the peptide loop had allowed additional modifications on the N184-glycan as evidenced by the appearance of a fully endoH-resistant species. Increased complex glycosylation of Δloop is also apparent from reduced electrophoretic mobility (Figure 3B). Thus, in the wt enzyme, the β-hairpin loop protects the N184-glycan from irregular processing, revealing the intimate connection of these two structural elements and lending additional support to the notion that ERGIC-53-binding is achieved by a single carbohydrate/peptide motif.

An Equivalent N-glycan/β-hairpin Loop Motif in Cathepsin C

Is the combined carbohydrate/peptide motif also present in another glycoprotein that is recognized by ERGIC-53, such as procathepsin C (Vollenweider *et al.*, 1998)? Like catZ, cathepsin C is a lysosomal papain protease. Maturation of procathepsin C involves splicing of the propeptide so that the very N-terminal segment, the exclusion domain, is part of the active, tetrameric structure. Strikingly, a characteristic β-hairpin loop has been found in the cathepsin C structure (Turk *et al.*, 2001) that shares many features with the ER-exit motif in procatZ. Like a forefinger, both hairpin loops project out of the globular structure without any spatial influence on the active site of the protease (Figure 7). Remarkably, the cathepsin C hairpin also teams up with a proximal N-glycan (Turk *et al.*, 2001) and the linear order of strand-loop-strand-glycosylation-site is identical to procatZ

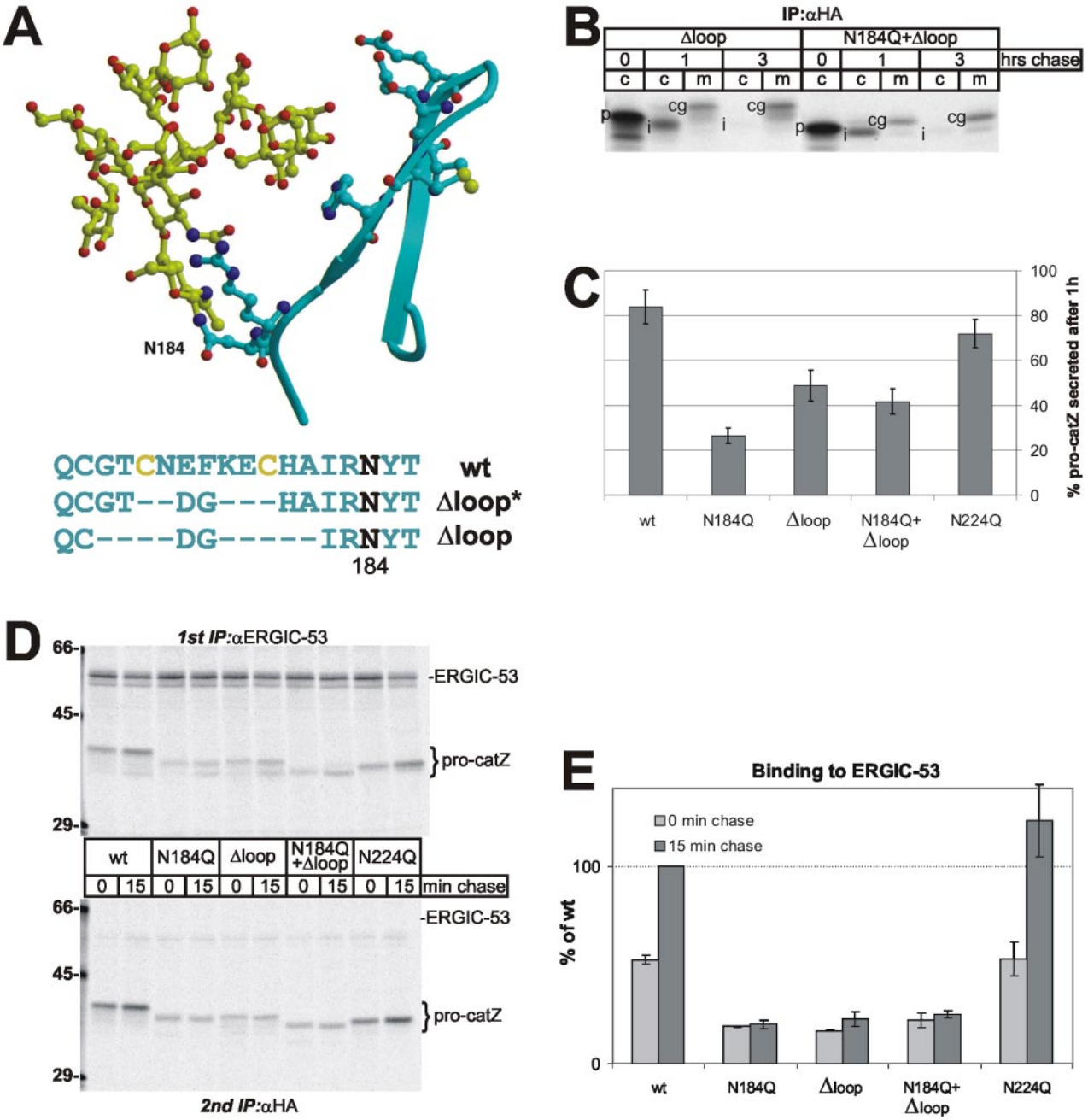

Figure 3. Efficient binding of procatZ to ERGIC-53 requires a combined carbohydrate/peptide motif. (A) Three-dimensional model of the peptide β-hairpin loop (cyan) and the high-mannose N184-linked glycan (yellow). The peptide structure was obtained from the protein data bank (PDB ID: 1DEU). The glycan is shown in a hypothetical conformation. Selected amino acid side chains that are likely to anchor the adjacent oligosaccharide by hydrogen bonds and the disulfide linkage are shown. As depicted in single letter code, mutations to eliminate the hairpin to the level of the disufide-linkage (Δloop*) or completely (Δloop) were engineered by introducing a DG-turn (corresponding to procatZ turns at positions 72/73, 252/253, or 282/283). (B) Secretion of Δloop and N184Q+Δloop (fluorogram). Transfected CHO cells were pulsed for 5 min, chased for different times, and analyzed by immunoprecipitation of HA-tagged procatZ from the cell lysate (c) or the medium (m). cg, complex glycosylated catZ; i, intermediate catZ; p, procatZ. (C) Quantification of initial (1 h) secretion of the glycan and Δloop mutants. The pulse-chase experiments were performed as in Figures 2A and 3B, and fluorograms were quantified by densitometric scanning. Means ± SD (n = 3). The reduction in secretion of N224Q is statistically not significantly different from wt as opposed to that of the other constructs. (D) Binding of glycan and Δloop mutants to GMAA-ERGIC-53. Sequential immunoprecipitation of GMAA-ERGIC-53 and recombinant procatZ (bottom panel) after a 10-min pulse with or without 15-min chase and DSP-treatment. The top panel shows 10% of the first (anti-ERGIC-53) immunoprecipitate. Molecular weight markers in kDa are indicated at the left margin. (E) Quantification of the binding of glycan and Δloop mutants to GMAA-ERGIC-53. The experiments were as in D. Fluorograms were quantified by densitometric scanning, normalized to ERGIC-53 (recovered in the first immunoprecipitation), and expressed as percentage of wt/15-min chase (mean ± SD, n = 3). ProcatZ mutants lacking the full carbohydrate/peptide motif exhibit weak binding that does not increase after 15-min chase.

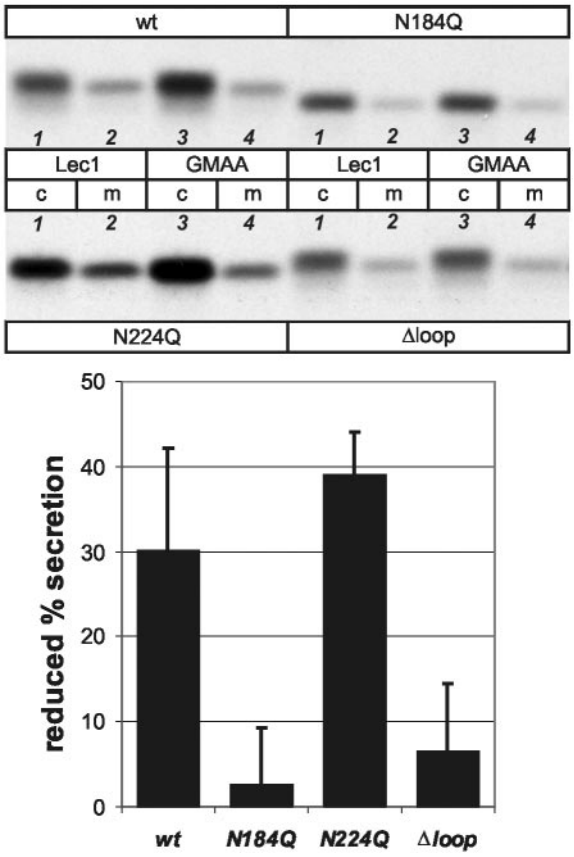

Figure 4. The full binding motif is required for the transport inhibition induced by GMAA-ERGIC-53. Comparison of the secretion of wt and mutant procatZ after 5-min pulse and 1-h chase from GMAA and Lec1 cells. Top: representative fluorograms. Bottom: quantification of the inhibition of secretion in GMAA versus Lec 1 cells (mean ± SD, n = 3). Calculation: 100[lane4/(lane3+lane4)]/[lane2/(lane1+lane2)]. Lane numbers are in italic. Note that only in the case of wt and N224Q the delay in secretion is statistically significantly different from zero ($p < 0.05$, Student's *t* test). c, cell lysate; m, medium.

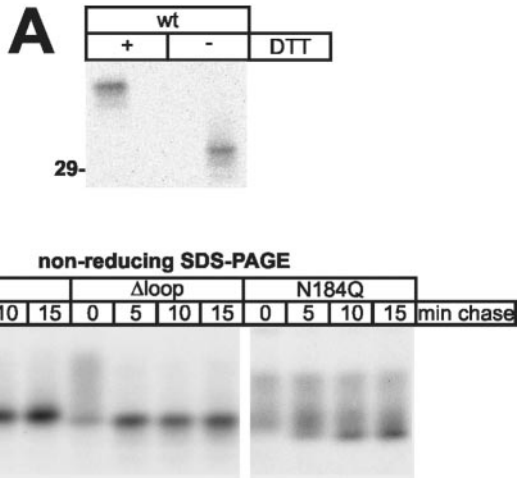

Figure 5. Folding kinetics of procatZ mutants. (A) CHO cells were transfected with wt-procatZ cDNA, pulsed for 5 min and chased for 15 min. ProcatZ immunoprecipitates were separated by SDS-PAGE in the presence or absence of dithiothreitol. The electrophoretic mobility of nonreduced procatZ is increased, because intramolecular disulfide bonds remain. The 29-kDa molecular-weight marker is indicated. (B) Pulse (5 min)-chase time course of procatZ mutants that were subjected to nonreducing gel electrophoresis after immunoprecipitation. Note that the conversion to a sharp band indicating the folded state is efficient in wt-procatZ and Δloop, but delayed in N184Q (fluorograms).

(Figure 1A) including the number of spacing amino acids. The carbohydrate-adjacent β-strand backbones can be superimposed with a rms deviation of 0.92 Å (Figure 7), suggesting that the exact 3D structure of this peptide may be important for lectin association. Unfortunately, in contrast to endogenous procathepsin C (Vollenweider *et al.*, 1998), the transport of transfected procathepsin C is minimally retarded by GMAA-ERGIC-53 and procathepsin C cannot be cross-linked to ERGIC-53 by DSP (unpublished data). Thus, procathepsin C is not amenable to the same analysis as procatZ.

DISCUSSION

The Transport Lectin Function of ERGIC-53

It is now widely assumed that receptor-mediated export of soluble cargo from the ER is an active process that concentrates cargo proteins into ER-derived vesicles and thereby increases their transport rate (Barlowe, 2003). The data of our study additionally suggest that receptor-mediated cargo selection at the level of ER-exit increases the fidelity of anterograde transport. Several considerations argue that we have indeed defined a mechanism of secondary quality control (Ellgaard and Helenius, 2003). First, we noted an increase in cargo-lectin binding after an initial lag-period that is characteristic for procatZ mutants harboring the full carbohydrate/peptide motif (Figure 3, D and E). Most impor-

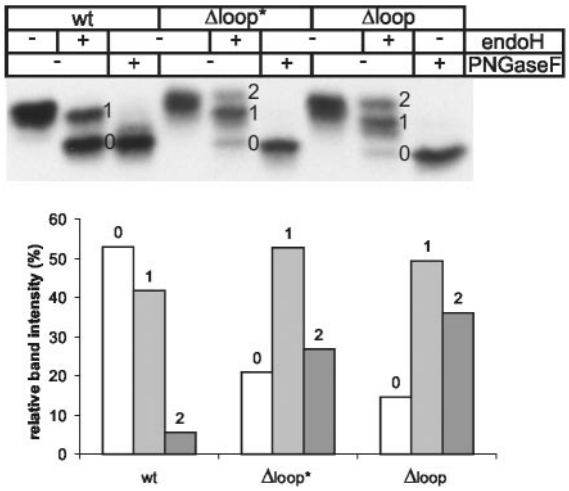

Figure 6. The β-hairpin loop protects the N184-glycan of procatZ from complex glycosylation. CHO cells transfected with wt-procatZ, Δloop*, and Δloop cDNA were pulsed for 5 min and chased for 3 h. Secreted procatZ was collected from the medium by anti-HA immunoprecipitation, probed for the sensitivity to endoH and PNGase F, and analyzed by SDS-PAGE/fluorography. Numbers indicate doubly-, singly-, and nonglycosylated procatZ after endoH treatment. The graph plots the percentages of endoH-resistant oligosaccharides for the three procatZ mutants as determined by densitometry.

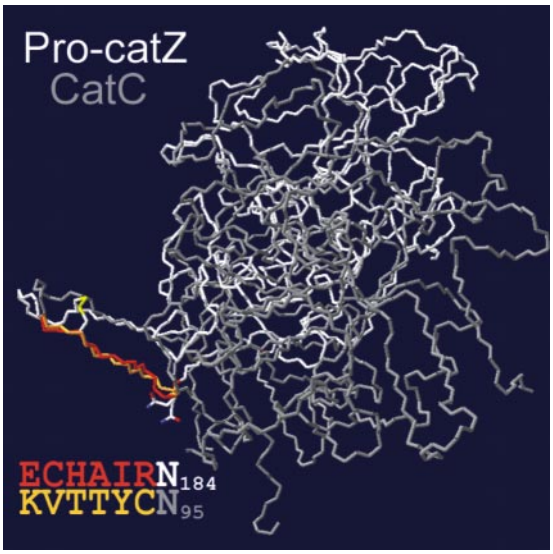

Figure 7. Superimposition of the hairpin loop motifs of procatZ and cathepsin C. The two highlighted hepta-peptides of procatZ (red) and cathepsin C (orange) were superimposed using the Swiss PDB viewer software (available at www.expasy.ch). Shown are the peptide backbones of procatZ (white, PDB ID: 1DEU) and cathepsin C (CatC, gray, PDB ID: 1K3B), the side chains of glycosylation-site asparagines 184 and 95, and the disulfide bridge within the procatZ hairpin. Note that the overlay is restricted to the β-hairpin loops. The full sequence of the cathepsin C motif is $\underline{K_{82}YKE}EG\underline{SKVTT}YCNET_{97}$ (β-strands are underlined; numbering according to Turk *et al.,* 2001).

tantly, in the case of wt procatZ this increase of binding is paralleled by folding (see Figure 5). These findings are consistent with the notion that only correctly folded procatZ, after release from the quality control machinery, is efficiently bound by ERGIC-53 and thereby competent to leave the ER. Second, glycoprotein binding to ERGIC-53 is affected by untrimmed glucose residues (Appenzeller *et al.,* 1999), which are known to play a major role in the calnexin/calreticulin cycle (Ellgaard and Helenius, 2003). Third, our discovery that ERGIC-53 recognizes a tertiary structure motif that is stabilized by an intrinsic disulfide linkage indicates that nonnative conformers of procatZ cannot present the proper ticket for ERGIC-53-mediated ER-exit. Taken together, the interaction of glycoproteins with the COPII-binding transport lectin ERGIC-53 appears to represent a quality control mechanism that acts complementary to the ER folding machinery and insures that preferentially folded cargo will be withdrawn from the folding environment of the ER by export.

Mutations in ERGIC-53 cause combined deficiency of coagulation factors V and VIII because of their inefficient secretion (Nichols *et al.,* 1998). Whether or not the coagulation factors V and VIII comprise a carbohydrate-adjacent β-hairpin is currently not known because of the lack of structural data. It is possible, however, that the transport assistance of ERGIC-53 to the coagulation factors occurs by a mechanism unrelated to the transport lectin activity described in the present study. Although high-mannose glycans play a role in the binding of coagulation factor VIII to ERGIC-53, binding also strongly involves protein-protein interaction (Cunningham *et al.,* 2003). Furthermore, although the interaction between procatZ and ERGIC-53 is so weak that it requires covalent cross-linking for efficient detection, coimmunoprecipitation of coagulation factor VIII with ERGIC-53 appears to be very robust. A genetic study has identified MCFD2 as a second protein implicated in the transport of coagulation factors V and VIII that is found in complex with ERGIC-53 (Zhang *et al.,* 2003). Whether or not MCFD2 also participates in the transport assistance of the cathepsins is currently under investigation.

An ER-exit Signal on Soluble Secretory Cargo

On the basis of their finding that the inhibition of ER glucosidases slows the transport of secretory glycoproteins, Lodish and Kong (1984) postulated that high-mannose glycans, after removal of glucose residues, may form part of the recognition site for a hypothetical ER-export receptor. Although the subsequent discovery of N-glycan–dependent folding in the ER has led to the notion that sugar-dependent transport of glycoproteins in many instances reflects ER quality control (Ellgaard and Helenius, 2003), the present study, 20 years later, finally confirms the Lodish and Kong prediction. Knowledge on transport signals in secretory proteins required for the recognition by specific receptors has remained poor (Barlowe, 2003). The secretory proteins invertase and Hsp150 of yeast appear to possess active sorting signals (Gaynor and Emr, 1997; Fatal *et al.,* 2004), but no cargo receptor has been identified yet. In the case of the yeast pheromone precursor glyco-pro-α-factor, Erv29p acts as an ER-export receptor (Belden and Barlowe, 2001). A number of structural features including N-glycosylation are required for efficient intracellular transport of pro-α-factor (Caplan *et al.,* 1991), but no link of these putative targeting motifs to Erv29p has been established.

In the present work, we have characterized a transport motif on procatZ that is composed of a sugar and a peptide determinant. It is obvious that the distinct secretion kinetics of the glycosylation-site- and Δloop-mutants of procatZ (Figure 3C) go together with their ability to bind ERGIC-53 (Figure 3E). It is generally difficult, however, to attribute the transport phenotype of a given mutant to the absence of positive transport signals and to exclude its retention by the quality control machinery. Importantly though, we document that the hairpin loop in procatZ is not essential for the efficient acquisition of the compact native fold (Figure 5B). Thus, the transport retardation of Δloop cannot be attributed to conformation-based retention in the ER, but appears to result from its poor capacity to bind ERGIC-53. In the case of the glycosylation-site mutant N184Q the interpretation is more complex. The fact that N184 + 224Q is completely retained in the ER and cannot be efficiently immunoprecipitated under native conditions (Figure 2A) is an indication of misfolding that may, to some extent, also include the single mutant N184Q. Consistent with this, the formation of native intramolecular disulfide bonds appears to be less efficient in this mutant (Figure 5B). On the other hand, folding of catZ does not strictly require oligosaccharide chains, as (nonglycosylated) bacterially expressed GST-catZ is enzymatically active (Santamaria *et al.,* 1998). In any case, the interaction between procatZ and ERGIC-53 depends on both carbohydrate and an intact carbohydrate recognition domain (Appenzeller *et al.,* 1999), and there is no doubt that the N184-glycan is part of the ER-export signal recognized by ERGIC-53. Interestingly, the N184-glycosylation consensus site is conserved from *Caenorhabditis elegans* to humans (Figure 1A), suggesting a pivotal targeting role for this oligosaccharide throughout the animal kingdom.

Similar to the procatZ, a β-hairpin loop close to an N-glycan is also found in cathepsin C (Figure 7). Interestingly, the β-hairpin loops appear to be evolutionarily unconnected despite the close relationship of the two cathepsins. Al-

though in procatZ the hairpin is contained in the papain domain, it is cathepsin C's exclusion domain that harbors this 3D motif. Moreover, the two amino acid sequences reveal no similarity apart from a tendency for charged side chains (Figure 7). These observations argue that the two loops arose independently by convergence. Furthermore, the lack of amino acid identity renders it unlikely that the hairpin loops directly associate with the lectin. We suggest that the loop motif functions by supporting an optimal conformation of the adjacent high-mannose glycan, which serves as an ERGIC-53 recognition motif. This notion is supported by the fact that the hairpin loop has a protective effect on the flanking N184-glycan later in the secretory pathway (Figure 6). Conformational support of carbohydrate chains by adjacent proteinaceous determinants might be a general mechanism that is fundamental for proper lectin-recognition. Many glycoproteins may present their oligosaccharide signals in a similar manner.

There may be a second contact area between procatZ and ERGIC-53. This is suggested by the fact that ~20% binding to ERGIC-53 remains in the absence of a functional N184-glycan/hairpin loop motif (Figure 3E) and that glycan-less procatZ weakly but reproducibly interacted with ERGIC-53 (Figure 2C). This second contact area may localize close to N224, because the binding of procatZ to ERGIC-53 slightly improves in the absence of the N224-glycan (Figure 3E). Interestingly, the glycan-independent interaction is already maximal after a short [^{35}S]methionine pulse and thus appears to be less conformation-selective than the glycan-dependent interaction. This notion is also supported by the observation that ERGIC-53 associates with N184Q immediately after a short pulse (Figure 3E) before this mutant has completed its folding (Figure 5B). Importantly, the binding of N184Q to ERGIC-53 did not further increase after longer chase times (unpublished data), demonstrating that this mutant—even when folded—entirely fails to interact in a carbohydrate-dependent manner. It should be noted that the levels of coprecipitation of N184Q, Δloop, and N184Q+Δloop with ERGIC-53, although relatively low, still by far exceed nonspecific coprecipitation (Figure 3D, top panel, and unpublished data). This second protein-protein interaction may reflect some transient association of incompletely folded procatZ and ERGIC-53 that is less stable than the lectin interaction and cannot promote ER-export. The function of this early association remains to be determined.

Oligosaccharide Processing in procatZ

Our data show that the N184 but not the N224-glycan remains endoH-sensitive during secretion. The endoH sensitivity of the N184-glycan critically depends on the presence of the hairpin loop that must be intact to prevent high-mannose trimming and complex glycosylation (Figures 3B and 6). We are currently testing the possibility that the protective effect of the hairpin loop during oligosaccharide processing is essential for mannose-6-phosphate–mediated targeting of procatZ to lysosomes.

It is worth noting that glycosylation enzymes of the Golgi and ERGIC-53 have opposite structural requirements for the recognition of the N184-glycan in procatZ. Although the Golgi enzymes can only modify the glycan in absence of the hairpin loop (presumably in a rather flexible state), ERGIC-53 can only recognize the glycan in the presence of the hairpin loop (presumably in a more rigid state). It is no surprise, therefore, that varying the length of the loop differentially influences these two unrelated processes. The intermediate deletion mutant Δloop* has no effect on ERGIC-53 recognition (unpublished data), but is prone to increased complex glycosylation on the N184-glycan (which, however, does not quite reach the level of complex glycosylation of Δloop; Figure 6).

In summary, we have identified the first ER-export motif on soluble secretory cargo. This motif consists of both a carbohydrate and a peptide determinant and is found in precise structural analogy on two glycoproteins, both of which interact with ERGIC-53 during anterograde transport from the ER. Our findings provide an explanation for the cargo selectivity of the mannose lectin ERGIC-53 in ER export. Whether the same mechanism underlies ER-export of blood coagulation factors V and VIII is currently unknown because the structure of these ERGIC-53 ligands has not been determined.

ACKNOWLEDGMENTS

We thank Käthy Bucher for technical assistance, Franziska Kuhn for helpful suggestions, Lorenza Bordoli for advice in biocomputing, Boris Turk for cathepsin C DNA, and Lars Ellgaard for critically reading the manuscript. The study was supported by the Swiss National Science Foundation (H.P.H.), the University of Basel (H.P.H.), the European Union (C.L.-O.), and the CICYT-Spain (C.L.-O.). I.S. is recipient of a Research Contract from Fondo deInvestigaciones Sanitarias (FIS 00/3161).

REFERENCES

Appenzeller, C., Andersson, H., Kappeler, F., and Hauri, H. P. (1999). The lectin ERGIC-53 is a cargo transport receptor for glycoproteins. Nat. Cell Biol. *1*, 330–334.

Appenzeller-Herzog, C., Roche, A. C., Nufer, O., and Hauri, H. P. (2004). pH-induced conversion of the transport lectin ERGIC-53 triggers glycoprotein release. J. Biol. Chem. *279*, 12943–12950.

Barlowe, C. (2003). Signals for COPII-dependent export from the ER: what's the ticket out? Trends Cell Biol. *13*, 295–300.

Belden, W. J., and Barlowe, C. (2001). Role of Erv29p in collecting soluble secretory proteins into ER-derived transport vesicles. Science *294*, 1528–1531.

Caplan, S., Green, R., Rocco, J., and Kurjan, J. (1991). Glycosylation and structure of the yeast MF alpha 1 alpha-factor precursor is important for efficient transport through the secretory pathway. J. Bacteriol. *173*, 627–635.

Cunningham, M. A., Pipe, S. W., Zhang, B., Hauri, H. P., Ginsburg, D., and Kaufman, R. J. (2003). LMAN1 is a molecular chaperone for the secretion of coagulation factor VIII. J. Thromb. Haemost. *1*, 2360–2367.

Dahms, N. M., and Hancock, M. K. (2002). P-type lectins. Biochim. Biophys. Acta *1572*, 317–340.

Ellgaard, L., and Helenius, A. (2003). Quality control in the endoplasmic reticulum. Nat. Rev. Mol. Cell. Biol. *4*, 181–191.

Fatal, N., Karhinen, L., Jokitalo, E., and Makarow, M. (2004). Active and specific recruitment of a soluble cargo protein for endoplasmic reticulum exit in the absence of functional COPII component Sec24p. J. Cell Sci. *117*, 1665–1673.

Gaynor, E. C., and Emr, S. D. (1997). COPI-independent anterograde transport: cargo-selective ER to Golgi protein transport in yeast COPI mutants. J. Cell Biol. *136*, 789–802.

Hauri, H., Appenzeller, C., Kuhn, F., and Nufer, O. (2000a). Lectins and traffic in the secretory pathway. FEBS Lett. *476*, 32–37.

Hauri, H. P., Kappeler, F., Andersson, H., and Appenzeller, C. (2000b). ERGIC-53 and traffic in the secretory pathway. J. Cell Sci. *113*(Pt 4), 587–596.

Herscovics, A. (2001). Structure and function of Class I alpha 1,2-mannosidases involved in glycoprotein synthesis and endoplasmic reticulum quality control. Biochimie *83*, 757–762.

Kappeler, F., Klopfenstein, D. R., Foguet, M., Paccaud, J. P., and Hauri, H. P. (1997). The recycling of ERGIC-53 in the early secretory pathway. ERGIC-53 carries a cytosolic endoplasmic reticulum-exit determinant interacting with COPII. J. Biol. Chem. *272*, 31801–31808.

Klemencic, I., Carmona, A. K., Cezari, M. H., Juliano, M. A., Juliano, L., Guncar, G., Turk, D., Krizaj, I., Turk, V., and Turk, B. (2000). Biochemical characterization of human cathepsin X revealed that the enzyme is an exopeptidase, acting as carboxymonopeptidase or carboxydipeptidase. Eur. J. Biochem. *267*, 5404–5412.

Kornfeld, R., and Kornfeld, S. (1985). Assembly of asparagine-linked oligosaccharides. Annu. Rev. Biochem. *54*, 631–664.

Lodish, H. F. (1988). Transport of secretory and membrane glycoproteins from the rough endoplasmic reticulum to the Golgi. A rate-limiting step in protein maturation and secretion. J. Biol. Chem. *263*, 2107–2110.

Lodish, H. F., and Kong, N. (1984). Glucose removal from N-linked oligosaccharides is required for efficient maturation of certain secretory glycoproteins from the rough endoplasmic reticulum to the Golgi complex. J. Cell Biol. *98*, 1720–1729.

Nichols, W. C. *et al.* (1998). Mutations in the ER-Golgi intermediate compartment protein ERGIC-53 cause combined deficiency of coagulation factors V and VIII. Cell *93*, 61–70.

Nufer, O., Kappeler, F., Guldbrandsen, S., and Hauri, H. P. (2003). ER export of ERGIC-53 is controlled by cooperation of targeting determinants in all three of its domains. J. Cell Sci. *116*, 4429–4440.

Sakamoto, E., Sakao, Y., Taniguchi, Y., and Yamafuji, K. (1999). Cathepsin Y (a novel thiol enzyme) produces kinin potentiating peptide from the component protein of rat plasma. Immunopharmacology *45*, 207–214.

Santamaria, I., Velasco, G., Pendas, A. M., Fueyo, A., and Lopez-Otin, C. (1998). Cathepsin Z, a novel human cysteine proteinase with a short propeptide domain and a unique chromosomal location. J. Biol. Chem. *273*, 16816–16823.

Schweizer, A., Fransen, J. A., Bachi, T., Ginsel, L., and Hauri, H. P. (1988). Identification, by a mAb, of a 53-kD protein associated with a tubulo-vesicular compartment at the cis-side of the Golgi apparatus. J. Cell Biol. *107*, 1643–1653.

Sivaraman, J., Nagler, D. K., Zhang, R., Menard, R., and Cygler, M. (2000). Crystal structure of human procathepsin X: a cysteine protease with the proregion covalently linked to the active site cysteine. J. Mol. Biol. *295*, 939–951.

Stanley, P., Caillibot, V., and Siminovitch, L. (1975). Selection and characterization of eight phenotypically distinct lines of lectin-resistant CHO cell. Cell *6*, 121–128.

Therrien, C., Lachance, P., Sulea, T., Purisima, E. O., Qi, H., Ziomek, E., Alvarez-Hernandez, A., Roush, W. R., and Menard, R. (2001). Cathepsins X and B can be differentiated through their respective mono- and dipeptidyl carboxypeptidase activities. Biochemistry *40*, 2702–2711.

Turk, D., Janjic, V., Stern, I., Podobnik, M., Lamba, D., Dahl, S. W., Lauritzen, C., Pedersen, J., Turk, V., and Turk, B. (2001). Structure of human dipeptidyl peptidase I (cathepsin C): exclusion domain added to an endopeptidase framework creates the machine for activation of granular serine proteases. EMBO J. *20*, 6570–6582.

Vollenweider, F., Kappeler, F., Itin, C., and Hauri, H. P. (1998). Mistargeting of the lectin ERGIC-53 to the endoplasmic reticulum of HeLa cells impairs the secretion of a lysosomal enzyme. J. Cell Biol. *142*, 377–389.

Zhang, B. *et al.* (2003). Bleeding due to disruption of a cargo-specific ER-to-Golgi transport complex. Nat. Genet. *34*, 220–225.